

Modeling and Simulation of Bearing Fault Response under Multivariable Conditions using MATLAB and Mathematical Formulation

Pravin Gosavi¹, Saniya Naik^{1*}, Vaishnavi Gavade¹, Nikita Chougule¹, and Sujal Kadam¹

¹Department of Mechanical, Kolhapur Institute of Technology's College of Engineering (Empowered autonomous) Kolhapur, Shivaji University, Kolhapur, Maharashtra, India - 416234.

Abstract. Rotating Machinery plays a crucial role across various industrial sectors. Bearings are the most crucial essential part that relies on various operations. Condition monitoring techniques have proven helpful in identifying the fault signatures that occur. This paper represents the vibration analysis of a SKF 6206 deep groove ball bearing. Predictive maintenance and scrutiny of a deep groove bearing under varying speeds, as well as defect size. To imitate the presence of faults, a localized defect of rectangular spall type is generated on the outer race of the bearing. Using the numerical simulation method, MATLAB default signatures are studied and compared with the experimental data obtained from the dedicated test rig. The graphs show the presence of default frequencies in the time domain and frequency domain, along with the effect of noise and vibration on them. The results show that the Numerical simulation method of using MATLAB has been proven useful, as it is time-efficient by reducing the need for an extensive procedure of experimentation and breakdown maintenance of that particular part in the industry.

1. Introduction

Bearings are a crucial component of every rotating machine, and the most widely used type is the Deep Groove Ball Bearing (DGBB). These bearings are used continuously across various industries due to their ability to withstand both radial and axial loads. The operation of a DGBB is continuous and should remain uninterrupted unless under proper supervision. Although they are rigidly built, prolonged use and exposure to harsh operating conditions or poor maintenance can cause them to deteriorate, eventually leading to failure. Bearing failures result in costly breakdown maintenance and can damage a company's reputation. Therefore, it is essential to operate and maintain bearings carefully to fully utilize their designed service life.

Extensive research is being carried out to minimize these functional losses as well as to predict the failure well in advance. By actually calculating it, the remaining useful life of a bearing can be known. Condition monitoring is the best approach to investigate the default

* Corresponding author: saniyanaik2005@gmail.com

frequency generated, which describes the condition of the bearing. Periodic Excitations are observed in the presence of faults like cracks, pits, and spalls on the rolling elements. These excitations are important markers of particular fault types because they appear in the vibration signal as discrete frequency components, such as Ball Pass Frequency Outer race (BPFO), Ball Pass Frequency Inner race (BPFI), Ball Spin Frequency (BSF), and Fundamental Train Frequency (FTF).

MATLAB is a numerical simulation method that is used to formulate the mathematical model that best describes our rotor bearing system. MATLAB is a powerful tool to describe the physics-based model and to describe the dynamic state of the test rig. It is a data-driven technique and is advantageous as it is time-efficient in calculating the results as compared to a traditional approach, which includes the experimentation of a bearing under various operating conditions. Not only is it a timely operation, but it is also very costly; one has to repeat the process for every iteration, as ideal conditions are to be maintained. Using MATLAB enables the user to develop an ideal environment and study the default frequency response curves.

This paper summarizes the use of MATLAB in diagnosing the faults along with the significant patterns developed by the vibration analysis which includes the time domain and frequency domain parameters which depicts the default signatures (peak amplitudes and peak frequencies). This information is used to understand and predict the nature of fault and its respective location for the bearing to be used until its complete life is utilized.

2. Literature review

Predicting the maintenance techniques have been revealing the industry revolution for a long time. Vibration monitoring is considered as the best approach for understanding the life of a bearing and predicting the possible failure of a bearing. Romanssini and Arguirre et al. [1] reviewed various aspects of bearing fault analysis for the understanding of the generated nature of vibrations which includes the sensors required to analyze the vibration in terms of displacement, velocity and acceleration spectrum, and the associated signal processing methods. They also concluded that vibration analysis is the gold standard technique and the usage of artificial intelligent and its algorithms has improved the fault diagnosis. They have also realized the challenges like the signal noise, sensor placements and differentiation of operating conditions in an actual working environment while reviewing. They recommend for better sensor fusion, creation of standard benchmark datasets and more field-validation trials to facilitate industrial deployment of research results.

Vibration-based condition monitoring for rotating machinery has been one of the important topics in the field of machinery health monitoring, as extensively reviewed by Tiboni et al. [2]. Their review indicates that vibration signals have the strongest ability to indicate mechanical faults, especially when modern signal processing techniques are applied. It was found that time-frequency and decomposition methods are able to obtain clearer fault characteristics under real operating conditions than traditional single-domain approaches. The review further points out that proper sensor placement and pre-processing may significantly reduce the noise and improve the diagnostic performance. With the aid of machine-learning and deep-learning, the automated fault identification in bearings, gears, motors and wind turbines is now dramatically improved.

Rolling element bearings have been an interesting subject for vibration-based fault diagnosis. Krishna and Vishwakarma [3] have done research on this. They found that the default frequencies show up better in the time domain analysis than in the frequency domain during their review. But when this domain is used to bring in new advancements and combine them with new approaches, it will perform more accurately and reliably for different operations.

Singh and his team have been looking closely at different ways to model bearing problems using vibration [4]. They have tried out many models, such as analytical, multi-body, and quasi-periodic ones. Along with this, they also did experiments that really helped them understand how defects in the bearings can cause vibrations. After watching everything carefully, they realized that while we do have ways to see some problems in bearings, we still need to make them better so they can work in the real world.

Randall [5] have presented a tutorial about the diagnosis of rolling element bearing using advanced signal processing. They have introduced separation methods (DRS, SANC) and enhancement tools (MED, spectral kurtosis) for extracting bearing fault signal that is masked by gear and shaft harmonics. Various case studies from high-speed turbine to slow rotating radar tower bearing has been demonstrated showing the flexibility of the framework. In conclusion, these methods along with the cyclostationary-based approaches should be used for early fault diagnosis.

Kim et al. [6] presented a MATLAB-based tutorial on envelope analysis for the diagnosis of rolling element bearings with focus on its incorporation in the PHM context. They underlined the importance of accurate vibration-signal processing in order to extract fault-related features in order to predict remaining useful life and presented a complete end-to-end workflow applied to an AR modelling, spectral kurtosis and STFT based demodulation band selection problem prior to the Hilbert based envelope analysis. They showed the successive steps of the proposed diagnosis workflow by using a simulated bearing signal and the extraction of fault frequencies. As a final step, they have validated the proposed methodology on the KAU test-rig data and the CWRU database and proved that it is a very efficient and effective workflow for beginners in vibration-based fault diagnosis.

MATLAB is a strong tool for working with data-based models and analyzing dimensions. It saves time and is useful when you study different ways of looking at vibrations, like time and frequency analysis. B. K. Pavan Kumar & Y. Basavaraj [7] used MATLAB's frequency analysis for predicting when spinning machines might need fixing. By changing vibration signals to graphs using state space models, they could connect the level of problem frequencies. The technique gives more than 85% accuracy in predicting machine health and checking its condition. They said such MATLAB tools can help make machines safer, make them stop less often, and help them last longer.

Prabhu et al. [8] made a math model to copy how the rotor bearing system works. He used this model to try out how vibration changes when a defect on the outer race moves. He applied Hertzian contact theory, nonlinear springs, and Runge-Kutta from MATLAB. The test got both time- and frequency-domain signatures. The defective bearing showed clear spikes and strong vibration amplitude. This model is good for finding small defects, and is a reliable predictive maintenance tool.

ADAMS MBS and MATLAB Simulink are two of the newest tools used to simulate models based on physics. Mishra et al. [9] used this method for studying a faulty bearing model and compared it to vibration signals. They created a 5-degree of freedom model that is quasi static for both good and bad bearings. They also did experiments on a real test rig. After doing a lot of research, they found that the ADAMS software's multi body model fits the real test results well and is reliable for simulation. But it is harder to compute and needs to be fine-tuned to match the actual tests. So, they said that faster analytical and quasi-static models should be used at first, and then ADAMS MBS should be used later for careful checking and setting up strong diagnostic tools.

Ma et al. [10] offered a dynamic simulation model for identifying faults when some fault type samples are missing. To produce fault signals, a rotor bearing simulation model of SKF 6203 was used and the simulated data was also mixed with the CWRU test data (SKF 6203/6205). The problem of incomplete fault datasets was solved by applying the WGAN-GN for data augmentation, and Stacked Autoencoders (SAE) is used for further classification.

By mixing the real signals with the GAN generated synthetic samples, the accuracy in identifying the bearing faults was improved. The results demonstrated that the simulations driven approaches are associated with the AI-based augmentation and are beneficial in tackling the lack of certain fault samples in real-world bearing diagnosis.

Table 1. Fundamental Parameters.

| | | | |
|-------------|---|------------|--|
| <i>DDBG</i> | <i>Deep groove ball bearing</i> | <i>dr</i> | <i>Ball diameter (mm)</i> |
| <i>BPF0</i> | <i>Ball pass frequency outer race (Hz)</i> | <i>z</i> | <i>Number of balls</i> |
| <i>BPFI</i> | <i>Ball pass frequency inner race (Hz)</i> | ϕ | <i>Contact angle</i> |
| <i>BSF</i> | <i>Ball spin frequency (Hz)</i> | <i>m</i> | <i>Mass (kg)</i> |
| <i>FTF</i> | <i>Fundamental train frequency (Hz)</i> | <i>c</i> | <i>Damping (Ns/m)</i> |
| <i>d</i> | <i>Bore diameter (mm)</i> | <i>k</i> | <i>Stiffness (N/m)</i> |
| <i>D</i> | <i>Outside diameter (mm)</i> | <i>F</i> | <i>Amplitude of external force (N)</i> |
| <i>DI</i> | <i>Shoulder diameter of the outer ring (mm)</i> | \ddot{x} | <i>Acceleration (m/s²)</i> |
| <i>F</i> | <i>Raceway diameter of the inner ring (mm)</i> | \dot{x} | <i>Velocity (m/s)</i> |
| <i>dp</i> | <i>Pitch diameter (mm)</i> | <i>x</i> | <i>Displacement (m)</i> |
| <i>B</i> | <i>Bearing Width (mm)</i> | <i>t</i> | <i>Time (s)</i> |

3. Model exploitation

3.1. Experimentation

A physical dynamic model was made which was installed with two end bearings, one drive end which was powered with the motor and other one is the non-drive end bearing which actually contributes in acquisition of vibration data. At this end, the testing deep groove ball bearings are installed in a sequence of increasing defect size from 0 mm defect i.e. healthy to faulty bearings. The actual vibration data was recorded on a computer with the help of accelerometer. A piezoelectric accelerometer (Deltron type 2524-B) with a sensitivity of 9.507 mV/g of Brüel and Kjær made with a peak measuring range of ± 714 g and a frequency range of 0.2 Hz to 12.8 kHz is used for vibration data collection. SKF6206 bearing is used for this experimental study. As seen earlier in the literature review the surface roughness of races of bearings affects the results in a significant way, so it is important to maintain the tolerance limit of surface roughness of the bearings.

Upon studying and considering the defect is located on the outer race, it has been come to acknowledge that the slow degradation of the balls on the races occurs in the form of spalls as a localised defect. To imitate this localised defect, a rectangular slot is created artificially on the outer race of the bearing using Electro-Discharge machining (EDM). This method maintains the accuracy level of the bearings as it can machine the slot up to micro levels. Along with the varying speeds, the defect sizes chosen for this experiment is 0 mm and 0.5mm wide and the depth is 1 mm throughout the thickness of the outer race.



Fig. 1. Actual Deep Groove Ball Bearing (SKF6206).

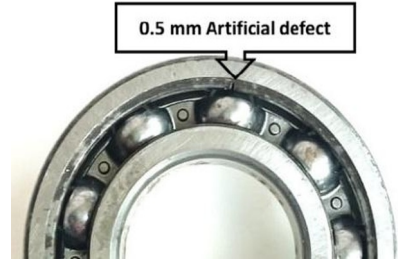


Fig. 2. Defective Bearing.

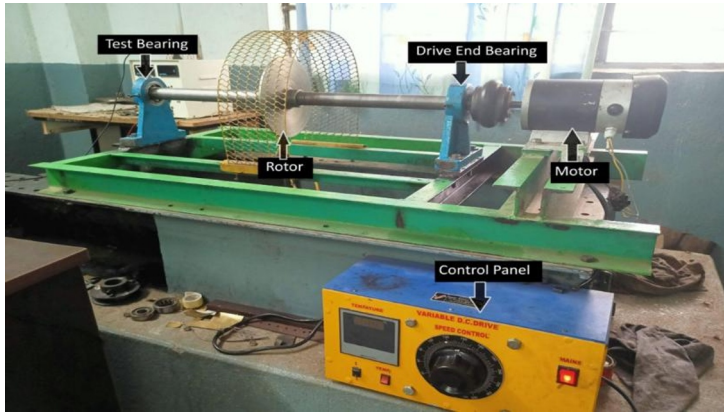


Fig. 3. Experimental Setup.

Table 2. Varying Defect Sizes and their Location.

| Defect Location | Defect Size |
|-----------------|------------------------------|
| Outer Race | 0 mm (Width) * 1 mm (Depth) |
| | 0.5mm (Width) * 1 mm (Depth) |

The data acquisition records the vibrational data which includes the patterns developed within the stipulated time intervals, the nature of response curve whether it is time dependent or frequency amplitude dependent, the intensity of those response curves and other size bands, along with the occurrences of defect frequency.

Table 3. Theoretical BPFO Calculations.

| Operating Speed (RPM) | Rotational Frequency in Hz (f_r) | $2f_r$ (Hz) | BPFO (Hz) | 2BPFO (Hz) | 3BPFO (Hz) | 4BPFO (Hz) |
|-----------------------|--------------------------------------|-------------|-----------|------------|------------|------------|
| 1200 | 20 | 40 | 71.41 | 142.82 | 214.23 | 285.64 |
| 1500 | 25 | 50 | 89.27 | 178.54 | 267.81 | 357.08 |

The occurrence of the defect is studied and calculated theoretically as well also known as BPFO. The BPFO is calculated theoretically, using the formula below to compare with experimental values. For example, the location of defect is on the outer race, the BPFO is (71.41, 89.27).

$$BPFO (Hz) = \frac{Z}{2} \left(1 - \frac{db}{dp} \cos \phi\right) f_r \dots \dots (1)$$

The actual test bearing (SKF6206) possesses certain parametric values that are listed in the table below and used for theoretical calculation. Also, these are most important when it comes for building of a robust mathematical model.

Table 4. Geometric parameters of SKF 6206 DGBB.

| Parameters | Values |
|--|----------|
| Bore diameter (d) | 30 mm |
| Outside diameter (D) | 62 mm |
| Shoulder diameter of the outer ring (D1) | 52.08 mm |
| Raceway diameter of the inner ring (F) | 37.5 mm |
| Pitch diameter (dp) | 46.48 mm |
| Bearing Width (B) | 16 mm |
| Ball diameter (dr) | 9.525 mm |
| Number of balls (Z) | 9 nos. |
| Net weight of bearing | 0.193 kg |
| Contact angle (\emptyset) | 0 deg |

3.2. Mathematical Modeling

Before diving into the simulation of our desired rotor bearing system, let us configure the mathematical formulation of this respective mathematical model to be constructed in MATLAB. The desired MATLAB model should satisfy the conditions of a real rotor bearing system, such as actuation of dynamic forces, along with time variation and in consideration of all the physical parameters of SKF6206 as discussed earlier. For a highly rotating bearing like component, even the smallest of defect creates impact force which will repeat periodically. Varying speeds impacts the occurrence of impact force as well. A combination of models is used for making a robust mathematical model along with a few assumptions to keep in mind.

- Gyroscopic effects of the shaft are neglected.
- Pure rolling is assumed between balls and raceways (no sliding).
- The outer race is fixed and does not contribute to dynamic motion.
- The defect geometry remains constant (no progressive wear).
- The model operates in a noise-free surrounding to isolate vibration effects of the fault.

3.2.1. Lagrangian Mechanics

This method is used for deriving the governing equations and it is most useful for our experimentation as it is cleaner and generalized for systems with constraints. It simplifies the equations for complex systems. This method captures the interactions between rotating as well as reciprocating motions. It is to be considered that our system has 6 DOF and multiple moving parts. It uses the Energy equation: $L=T-V$ (2)

$$\text{Kinetic Energy (T)} = \frac{1}{2} \times m\dot{x}^2 \quad \dots\dots\dots (3)$$

$$\text{Potential Energy (v)} = \frac{1}{2} \times kx^2 \quad \dots\dots\dots (4)$$

By applying Euler langrage equation we get,

$$m\ddot{x} + cx + kx = F(t) \quad \dots\dots\dots (5)$$

3.2.2. Ordinary Differential Equation (ODEs)

This method was implemented in order to compute the vibration displacement over time and solvers like ode45 are adaptive with Runge-Kutta. The system is time dependent, so this

approach is most contributing to the study as the impact generated by the presence of the slot varies with time. Signals generated by the faults are dynamic and are best captured by ODEs. The varying speeds and external loads also describe the system response. The ODEs are defined in the form of:

$$\dot{X} = f(X, t) \quad \dots \dots (6)$$

3.2.3. Runge kutta method (4th Order)

In order to solve the ordinary differential equation, we need to use the numerical solution method, nothing but the Runge-Kutta method. It uses the built in solvers like ode45 of 4th order to solve the system's equations which vary with time. It is more accurate and stable of them all. Also, it is very efficient in handling the time varying forces like BPFO. It computes the displacement of Vibration i.e. $x(t)$ over the time. This system continuously updates the displacement vector and computes the forces including forces.

3.2.4. Dimension Analysis

This method is used to simplify the process by actually feeding the system with multiple parameters, like the mass of the bearing, its stiffness etc., with proper units. The dimensional analysis reduces the number of variables wherever possible and checks the consistency. The units ensure that the system is balanced. This plays an important role as the system is totally computational, and relies on the true information of the bearing. It also helps to create the non-dimensional groups like natural frequency which helps to generalize the results across system.

3.3. Numerical Solution (MATLAB)

By using the above given mathematical formulation, a suitable code is generated in order to perform this experiment though numerical solution method, we followed her is MATLAB. By incorporating the necessary values mentioned in the table 4, the solver in the MATLAB is solves the equations of the system and its output is seen in time domain analysis. The generation of amplitudes over a period of time, with specific time steps, is called time domain analysis. Using the FFT analyzer, we convert the time domain data into the frequency domain data, which is to check the vibration pattern created by the bearing. By applying the Hilbert transform, this data is converted into envelope analysis to signify the peaks and understand their nature. For study purpose a selective sampling frequency and set of data points is used. The vibration pattern holds a lot of coordinates which describes various statistical feature values, like peak values, peak amplitudes, crest factor, kurtosis, skewness, etc. these values are helpful whenever the system will be upgraded to Machine learning.

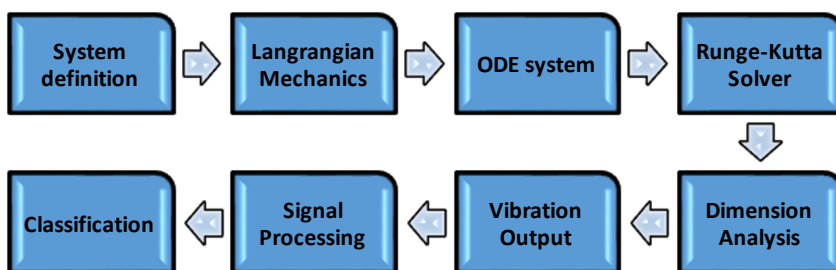


Fig. 4. Flow of Methodology.

4. Results and Discussion

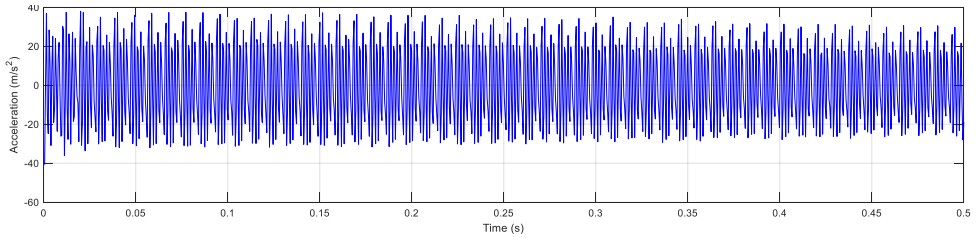


Fig. 5. Time Domain Graph using MATLAB at 1200 rpm of Healthy Bearing.

The graph in the time domain displays a steady and continuous waveform of vibrations, which is common for a healthy bearing running at 1200 rpm. The signal displays regular and smooth oscillations, with no sudden spikes or impulsive peaks, which suggests that there are no localized defects present. The amplitude of the vibrations is consistent throughout the entire 0.5-second time span, indicating uniform rotation and stable dynamic behavior. This type of waveform is usually observed in undamaged bearings where there are no impact forces generated during operation.

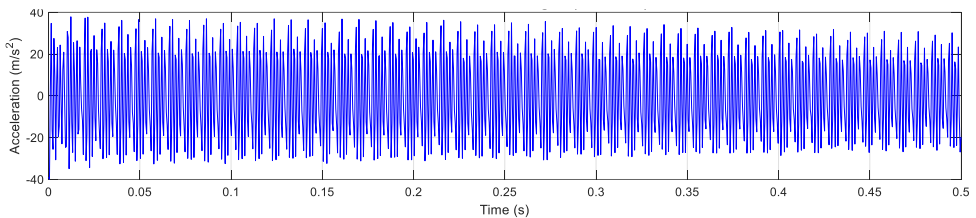


Fig. 6. Time Domain Graph using MATLAB at 1200 rpm of 0.5mm Defective Bearing.

Periodic spikes are seen in the time response. They are caused by the rolling elements passing a local defect of 0.5 mm on the outer race. Each time the bearing components make contact with the defect, there is an impulsive acceleration response followed by a decay due to system damping. The rise–decay pattern is repeated throughout the 0.5 s duration, which suggests that contact is being made with the defect once per revolution. The spiky waveform compared to the healthy bearing confirms defect-induced changes in vibration behavior at 1200 rpm.

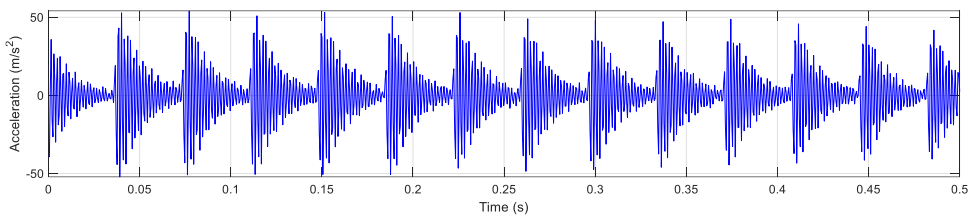


Fig. 7. Time Domain Graph using MATLAB at 1500 rpm of Healthy Bearing.

The waveform in the time domain shows even, recurring modulation patterns that are typical for a healthy bearing at 1500 rpm. There are no sudden bursts or sharp changes in the amplitude, which means there are no local faults. The amplitude rises and falls in a steady way because of the normal modulation that comes from how fast it's spinning and resonance. The vibration response is pretty steady and stable during the 0.5 s. This is normal for a bearing in good shape.

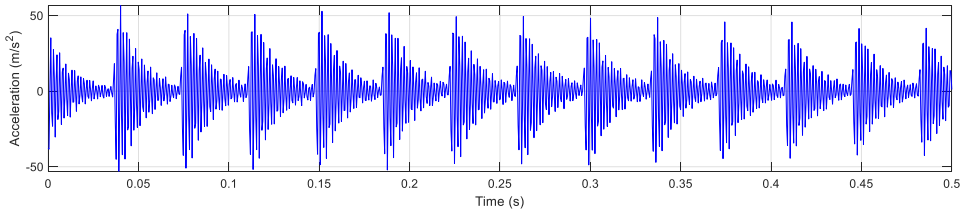


Fig. 8. Time Domain Graph using MATLAB at 1500 rpm of 0.5mm Defective Bearing.

The signal in the time domain displays clear, periodic spikes that happen when the rolling elements go over the 0.5 mm outer race flaw at 1500 rpm. At each spot of damage, a sharp, high spike shows up, followed by a decaying pattern in vibration from the system's damping effect. This repeated pattern makes the modulated waveform you see over the 0.5-second time. When you compare it to a healthy bearing, strong spikes show that defect-induced vibration is happening because of the outer race damage at this speed.

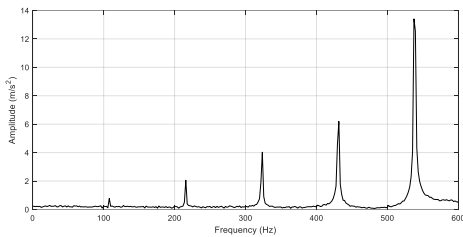


Fig. 9. Frequency Domain Graph using MATLAB at 1200 rpm of Healthy Bearing.

The spectrum displays clear harmonic peaks with amplitudes that get larger as the frequency increases. You can see sharp spikes at about 2 m/s², 4 m/s², and 6–8 m/s², with the highest peak reaching around 14 m/s² at the highest harmonic. The SKF 6206's BPFO at a speed of 1200 rpm (20 Hz) is 71.41 Hz. There is not a strong spectral peak at, or near, 71.41 (or the frequencies of the harmonics of 71.41). This suggests that there is not a localized outer-race defect. The noise floor in the spectrum is low, the harmonics progress smoothly without any obvious sidebands and the low-frequency harmonics of shaft-speed are weak. This is a healthy bearing.

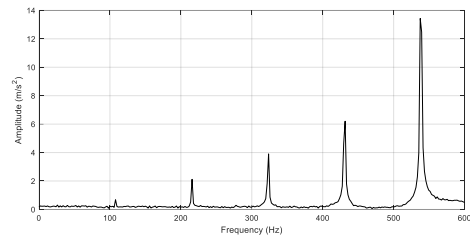
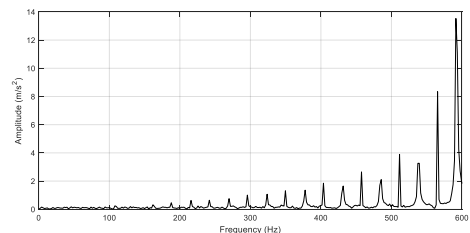


Fig. 10. Frequency Domain Graph using MATLAB at 1200 rpm of 0.5mm Defective Bearing.

The spectrum has more tiny spikes next to the calculated BPFO 71.41 Hz, which shows the existence of an outer raceway defect. The noise floor is slightly higher, and more defect-related components showed up in the lower frequency range compared with that of the healthy bearing. The harmonics around 150 Hz, 300 Hz, 450 Hz, and 600 Hz carry the main energy with their amplitudes increasing stepwise to about 2, 4, 6–8, and 14 m/s². All these distortions and added side peaks indicate periodic impacts of the rolling element passing the 0.5 mm spall. This spectrum also shows obvious fault-induced energy, which differentiates the defective bearing from the healthy one.

Fig. 11. Frequency Domain Graph using MATLAB at 1500 rpm of Healthy Bearing.



There are no BPFO frequency peaks in the spectrum for the healthy bearing measured at 1500 rpm. This confirms the lack of an outer-race defect. Only shaft-related harmonics are present, which appear as a group of closely spaced peaks whose amplitudes begin at less than 2 m/s^2 and slowly increase as the frequency approaches the higher-frequency region. A concentrated group of harmonics is present at about the 500–600 Hz region, where the amplitudes suddenly increase to about $12\text{--}14 \text{ m/s}^2$. The noise floor is constant and low throughout the spectrum. No defect-signature sidebands are present. The overall plot is smooth and typical of a healthy bearing with no sign of BPFO-related damage.

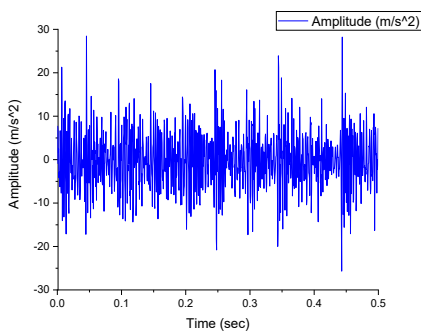


Fig. 12. Experimental Time Domain Graph at 1200 rpm of Healthy Bearing.

The time-domain vibration response of a healthy bearing working at 1200 rpm is shown in Figure. The waveform maintains a random, noise-like character without notable periodic impact forces, with the vibration amplitude varying between approximately $\pm 20 \text{ m/s}^2$. The absence of sharp impulsive peaks and periodic shock signatures confirms that the rolling motion is in good contact. The overall signal appears as typical broadband mechanical noise from a healthy bearing under steady-state rotation.

The spectrum displays a pronounced harmonic series spaced at the $\text{cBPFO} = 89.47 \text{ Hz}$, which supports the diagnosis an outer-race defect. Individual amplitude peaks originate just below 2 m/s^2 and ramp upwards toward the higher harmonics. Several harmonics are present at about 90, 180, 270 and 360 Hz and beyond, with each stronger than the last. The largest peaks in the region just below 550–600 Hz have amplitudes greater than 12 m/s^2 . The highest-level response is presumably due to the fault. Overall, the resolution of so many harmonics, combined with the increasing amplitude trend of successive harmonics, leaves little doubt about the existence and severity of the 0.5 mm outer-race fault.

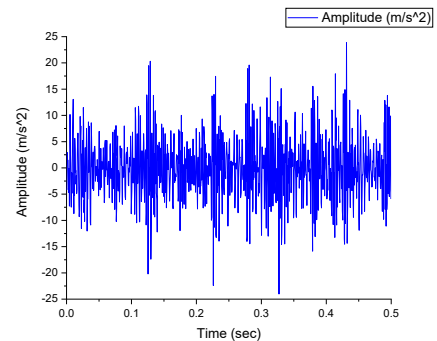


Fig. 13. Experimental Time Domain Graph at 1200 rpm of 0.5mm Defective Bearing.

The signal in the time domain at 1200 rpm for the 0.5 mm defect in the outer race has clear impulsive peaks on the normal vibration. These impacts happen regularly as the rolling elements hit the defect. This causes sharp spikes that go up and down, reaching about $\pm 25 \text{ m/s}^2$. If you compare this to a healthy bearing, the waveform has bigger changes and more random shock events. This shows higher mechanical activity. The repeated sharp bursts show there is a fault and the bearing is not smooth anymore. This is a typical vibration response from outer race defects.

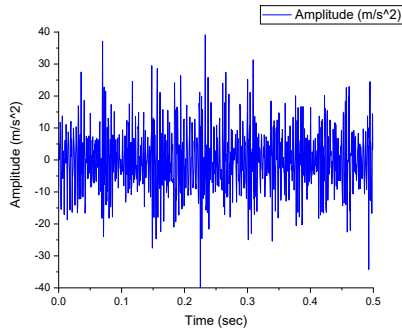


Fig. 14. Experimental Time Domain Graph at 1500 rpm of Healthy Bearing.

At 1500 rpm, the healthy bearing's time-domain signal shows a stable vibration and does not have any impact signature that is observed periodically on the time axis. Its waveform is also confined to around ± 35 m/s². It does not have any sudden spikes, asymmetry, or repeated shock pulses, which proves that the rolling elements are healthy. This noise-like random pattern is the usual broadband vibration observed from a bearing that is not faulty. In summary, this graph shows a mechanically healthy system without any sign of any kind of localized defects.

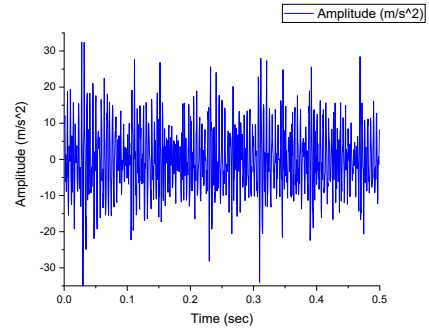


Fig. 15. Experimental Time Domain Graph at 1500 rpm of 0.5mm Defective Bearing.

The waveform for the 1500 rpm time range has obvious impact-type vibrations, which are a sign that the outer race is broken. The shocks that happen when the roller hits the 0.5 mm pit can be seen as sharp negative-going spikes that reach almost -40 m/s² and as high positive peaks that happen from time to time. Compared to the healthy bearing, which had a smaller range of amplitude, the broken bearing has a larger and more unpredictable range, which shows that it is becoming less mechanically stable. The repeated high-energy impulses that are buried in the noise show that there is damage in a small area. The broken bearing signal as a whole shows that the impact is getting worse because of the higher speed and the spread of defects.

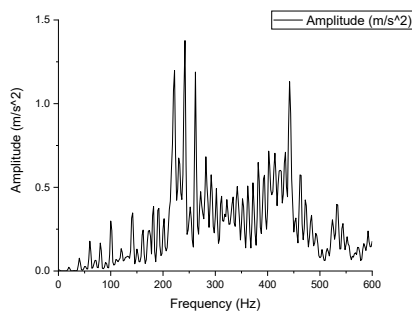


Fig. 16. Experimental Frequency Domain Graph at 1200 rpm of Healthy Bearing.

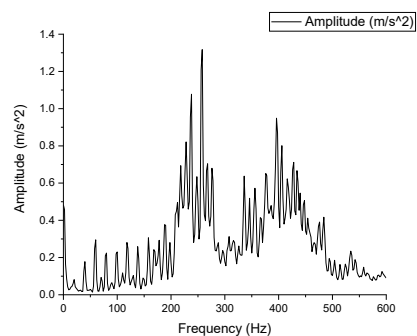


Fig. 17. Experimental Frequency Domain Graph at 1200 rpm of 0.5mm Defective Bearing.

The FFT plot for 1200 rpm, i.e. 20 Hz shaft speed, is of a broadband vibration spectrum. The dominant part of the energy is distributed around 200–450 Hz and is typical for a healthy bearing with the normal operating load. It is clear from the plot that there are no well-defined fault-frequency peaks, e.g. the BPFO (71.41 Hz), which confirms that the bearing has no outer-race damage. The amplitude values are rather low, with maximum peaks around 1.0–1.2 m/s^2 , which indicates that the dynamic conditions are stable. The spectrum is typical for a normal bearing operation, there is no modulation due to a fault and therefore, no harmonic signatures.

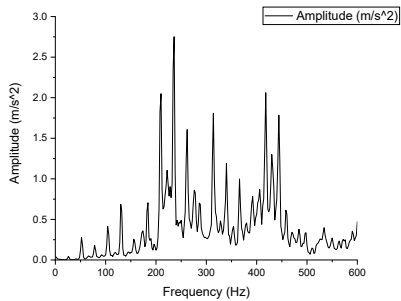


Fig. 18. Experimental Frequency Domain Graph at 1500 rpm of Healthy Bearing.

The figure shows the FFT spectrum from a test of a healthy bearing running at 1500 rpm. The BPFO here is 89.47 Hz. The graph shows that the vibration is low and stable. Most of the time the vibration is below 2.5 m/s^2 . This means there is no defect. Most of the high peaks are close to the shaft frequency (25 Hz) or its harmonics. This kind of pattern is normal for a good bearing running like normal. There are no big peaks at 89.47 Hz or its harmonics. This proves there is no fault. In short, the spectrum shows defect-free and smooth bearing operation with no modulation effects.

The frequency spectrum at 1200 rpm, the spectrum is dominated by the clearly discernible peaks at around 200–260 Hz due to the rich vibration components caused by the 0.5 mm defect. The calculated BPFO, 71.41 Hz, and its harmonics (2x, 3x, 4x) seem to be superimposed on the broadband energy rise. The amplitude levels reach approximately 1.2 m/s^2 , much higher than the healthy-bearing case. The dense group of sharp peaks around the mid-band is consistent with periodic outer-race impacts. Overall, the spectrum demonstrates clear defect-induced modulation with a high level of vibration severity.

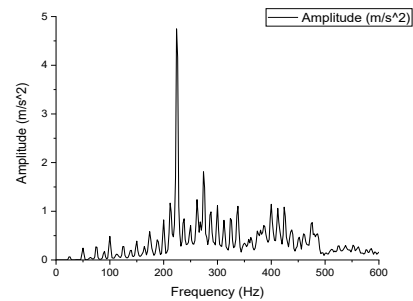


Fig. 19. Experimental Frequency Domain Graph at 1500 rpm of 0.5mm Defective Bearing.

The FFT test at 1500 rpm has a main spectral peak close to the predicted BPFO of 89.47 Hz, which is caused by periodic impacts created by an outer race defect. There's a strong, narrow spike almost at 5 m/s^2 , showing a high-energy shock response from the 0.5mm pit. We can also see several harmonic parts and modulation sidebands with BPFO near it, which happen because of amplitude and frequency modulation because of the roller-defect interaction. The broadband noise floor is much higher, showing that structural excitation has increased. The pattern of harmonics also shows the defect has expanded. Basically, the spectrum shows an obvious outer race localized fault.

Table 5. Statistical Features.

| Defect (mm) | Speed (RPM) | RMS | Peak Value | Peak Factor | Crest Factor | Kurtosis |
|-------------|-------------|-------|------------|-------------|--------------|----------|
| 0 | 1200 | 0.34 | 1.38 | 4.05 | 4.05 | 4.16 |
| | 1500 | 0.54 | 2.75 | 5.05 | 5.05 | 8.34 |
| 0.5 | 1200 | 0.344 | 1.32 | 3.83 | 3.83 | 2.480 |
| | 1500 | 0.53 | 4.75 | 8.87 | 8.87 | 57.95 |

To clearly compare the dynamic responses between healthy and defective bearings, we use many usual statistic features in time domain, such as RMS, Peak Value, Peak Factor, Crest Factor and Kurtosis, extracted from the measured vibration signals. RMS is the total vibration energy, only slightly changed for two bearing conditions in 1200rpm, it is because RMS is not very sensitive for small localized defect situation. The Peak Value increased a lot in defective bearing, especially in high speed, like 4.75m/s² when 1500rpm, shows high amplitude transients generated by the roller–defect repetitive impacts. This behavior is also represented in the Peak Factor, which is the same result for Crest Factor. Crest Factor and Peak factor both give a large increase in the defective condition, which evidence the impulsive and non-stationary nature of the resulting waveform. Among all these features, Kurtosis is the most discriminative one, showing a sharp increase of 8.34 to 57.95 at 1500rpm, from healthy to defective bearing condition, revealing the statistical prominence of repetitive shock impulses from the outer-race pit. These features could well describe the defect condition vibration signal and increase the feature separability for the SVM classifier, thus enhance the reliability and accuracy of the fault detection.

5. Conclusion

The graphical representations show that the generated graph is periodic as the ball returns on that same position after one rotation, so this pattern repeats itself after certain time intervals. The effect of noise in the surrounding creates the side bands around the spikes. As compared to the experimental graphs it can be seen that the assumptions made in the MATLAB tempt the graph to exclude the sidebands and enhance the spikes only. The Time domain graphs show the decaying curve which repeats after a certain time interval. Along with that the frequency spectrum shows the occurrence of defect on the outer race and its repetition into multiples of the calculated theoretical calculation. Not just that the frequency curve expands as the speed increases. Also, the dampening effect is observed, as the material is removed the stiffness decreases. Whereas the smaller defect dampens the vibration curve. Upon studying the frequency curves in both time domain and frequency domain, it can be said that the rotating element will eventually start pitting of surface and thereby reducing the material on the outer race and creating a rectangular spall.

Acknowledgement

The authors express their sincere appreciation to all those who contributed to the successful completion of this research titled “Modelling and Simulation of Bearing Fault Response under Multivariable Conditions using MATLAB and Mathematical Formulation”. Special thanks are extended to Dr. R. G. Desavale for his exceptional guidance, continuous encouragement, and invaluable support throughout the course of this work. His expertise in rotor dynamics and machine learning, along with his effective feedback, played an important role in the process of this project outcome. I also extend my heartfelt thanks to the Department of Mechanical Engineering for providing the necessary facilities and resources to carry out this project effectively. Special thanks to my friends for their cooperation, assistance, and motivation at various stages of this work which enabled me to complete this project smoothly.

Reference

1. Romanssini, Marcelo, et al. "A review on vibration monitoring techniques for predictive maintenance of rotating machinery." *Eng* 4.3 (2023): 1797-1817.
2. Tiboni, Monica, Carlo Remino, Roberto Bussola, and Cinzia Amici. 2022. "Applied Sciences A Review on Vibration-Based Condition Monitoring of Rotating Machinery."
3. Krishna, BM Vamsi, and Manish Vishwakarma. "A review on vibration-based fault diagnosis in rolling element bearings." *International Journal of Applied Engineering Research* 13.8 (2018):
4. Singh, Sarabjeet, Carl Q. Howard, and Colin H. Hansen. "An extensive review of vibration modelling of rolling element bearings with localised and extended defects." *Journal of Sound and Vibration* 357 (2015): 300-330.
5. Randall, Robert B., and Jerome Antoni. "Rolling element bearing diagnostics—A tutorial." *Mechanical systems and signal processing* 25.2 (2011): 485-520.
6. Kim, Seokgoo, Dawn An, and Joo-Ho Choi. "Diagnostics 101: A tutorial for fault diagnostics of rolling element bearing using envelope analysis in matlab." *Applied Sciences* 10.20 (2020): 7302.
7. Kumar, BK Pavan, and Yadavalli Basavaraj. "Vibration Analysis of Frequency Domain Data using MATLAB for Application of Rotating Part Machines in Industry." 10(1):1–5 (2023).
8. Prabu, J., et al. "Mathematical simulation of vibration signature of ball bearing defects in a rotor bearing system." *IOP Conference Series: Materials Science and Engineering*. Vol. 912, No. 2. IOP Publishing, 2020.
9. Mishra, Chintamani, Arun Kumar Samantaray, and Goutam Chakraborty. "Ball bearing defect models: A study of simulated and experimental fault signatures." *Journal of Sound and Vibration* 400 (2017): 86-112.
10. Ma, Junqing, et al. "Dynamic simulation model-driven fault diagnosis method for bearing under missing fault-type samples." *Applied Sciences* 13.5 (2023): 2857.